CHEMISTRY
A European Journal

A Journal of
ChemPubSoc Europe

Accepted Article

Title: N-Heterocyclic Carbene-Modified AuPd Alloy Nanoparticles and their Application as Biomimetic and Heterogeneous Catalysts

Authors: Patricia Tegeder, Matthias Freitag, Kathryn Chepiga, Satoshi Muratsugu, Nadja Möller, Sebastian Lamping, Mizuki Tada, Frank Glorius, and Bart Jan Ravoo

To be cited as: *Chem. Eur. J.* 10.1002/chem.201803274

Link to VoR: http://dx.doi.org/10.1002/chem.201803274

Supported by
ACES

WILEY-VCH

10.1002/chem.201803274

WILEY-VCH

N-Heterocyclic Carbene-Modified AuPd Alloy Nanoparticles and their Application as Biomimetic and Heterogeneous Catalysts

Patricia Tegeder,[a,+] Matthias Freitag,[a,+] Kathryn M. Chepiga,[a] Satoshi Muratsugu,[b] Nadja Möller,[a] Sebastian Lamping,[a] Mizuki Tada,[b,c] Frank Glorius,[a,*] and Bart Jan Ravoo[a,*]

Abstract: Herein we present the preparation of water soluble, N-heterocyclic carbene-stabilized AuPd alloy nanoparticles by a straightforward ligand exchange process. Extensive analysis revealed excellent size retention and stability over years in water. The alloy nanoparticles were applied as biomimetic catalyst for the aerobic oxidation of D-glucose, in which monometallic Au and Pd nanoparticles showed no or negligible activity. The alloy nanoparticles were further applied as titania-supported heterogeneous catalysts for the mild hydrogenation of nitroarenes and in the semihydrogenation of 1,2-diphenylacetylene with a solvent-dependent selectivity switch between *E*- and *Z*-stilbene.

Introduction

Catalysts based on transition metal nanoparticles (NPs) have received significant attention in recent years due to their unique catalytic activity and selectivity.[1] Their properties and catalytic performance strongly depend on size, shape, ligand shell and metal core composition. Bimetallic NPs are of particular interest, since they do not only combine the characteristics of their monometallic correspondents, but often also feature new properties due to synergistic effects between the two elements.[2] This can lead to enhanced catalytic performance, new selectivities and better colloidal stability. One of the best investigated bimetallic NP systems are AuPd alloy NPs, which exhibit catalytic activity in a wide range of reactions.[3] Au and Pd are miscible in all ratios, so that the reactivity of the alloy NP can be easily tuned by adjusting its metal composition. Besides the NP core itself, the adsorbed stabilizing ligands on the metal surface play a crucial role in the catalytic reactivity and selectivity. In the last few years, N-heterocyclic carbenes (NHCs) have gained increasing attention as ligands for transition metal nanoparticles due to their inherent electron-richness and structural diversity.[4-6] Until now, NHCs have been mainly applied for the stabilization of monometallic Au-,[7] Pd-,[7d,7g,7h,8] Pt-,[9] and RuNPs.[10] Very recently, Glorius et al. reported the surface modification of supported Ru/K-Al_2O_3[11] and Pd/Al_2O_3[12] with NHC ligands. The coordination of the carbenes on the metal NPs enabled the tuning of their chemoselectivity or even induced reactivity.

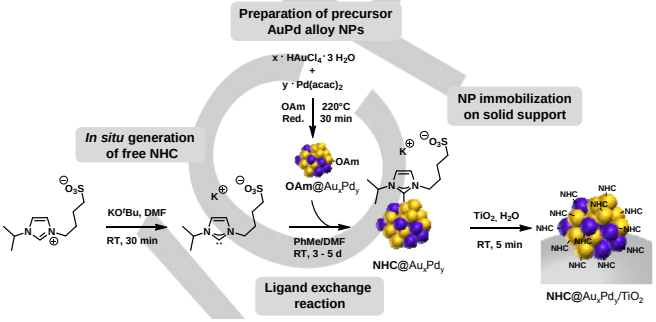

Scheme 1: Preparation of the NHC modified AuPd alloy NPs and their subsequent immobilization on TiO_2.

Previously, we reported the development of several innovative NHC ligand systems for the stabilization of Au- and PdNPs, with the latter being highly active in the chemoselective hydrogenation of olefins.[7g,7h,8a] This previous work focused mainly on the tailoring of the NHC's chemical structure to *1)* design effective stabilizers to prevent NP aggregation and *2)* to tune the NPs solubility to enable catalysis in different reaction media. Having this structural and electronically versatile library of NHC ligands in hand, our ongoing research is focusing on the functionalization of other interesting NP systems to realize a broader range of applications.[13] In this work, we focused on combining bimetallic alloy systems with the advantageous properties of a supported heterogeneous system. To the best of our knowledge, this is the first time bimetallic metal NPs have been functionalized with NHC ligands. We chose AuPd alloy NPs for examination since our previously described NHC ligands bind to both Au- and PdNPs and we therefore assumed they would also strongly coordinate to their bimetallic mixture. For comparison, three different Au-rich metal compositions ($Au_{95}Pd_5$, $Au_{90}Pd_{10}$ and $Au_{75}Pd_{25}$) were employed to investigate the effect of the element ratio on the NP properties and catalytic performance. The alloy NPs were functionalized with the NHC ligand before immobilizing them on the support to enable their characterization in solution (e.g. by NMR). For a strong adsorption of the alloy NPs on the support material, we utilized an anionic NHC ligand bearing a sulfonate group as a stabilizer. The most commonly used supports are made of metal oxides providing a charged surface. Thus, we reasoned that the electrostatic interaction between the sulfonate group and the support surface would enable the irreversible immobilization of the alloy NPs.

Results and Discussion

Nanoparticle Preparation

[a] Dr. P. Tegeder, M. Freitag, Dr. K. M. Chepiga, N. Möller, S. Lamping, Prof. Dr. F. Glorius, Prof. Dr. B. J. Ravoo
Westfälische Universität Münster
Organisch-Chemisches Institut
Corrensstrasse 40, 48149 Münster (Germany)
E-Mail: glorius@uni-muenster.de, b.j.ravoo@uni-muenster.de
[b] Prof. Dr. S. Muratsugu, Prof. Dr. M. Tada
Nagoya University
Department of Chemistry, Graduate School of Science,
[c] Research Center for Materials Science (RCMS), and Integrated Research Consortium on Chemical Sciences (IRCCS),
Furo-cho, Chikusa, Nagoya, Aichi 464-8602 (Japan)

[+] These authors contributed equally to this work.

Supporting information for this article is given via a link at the end of the document.

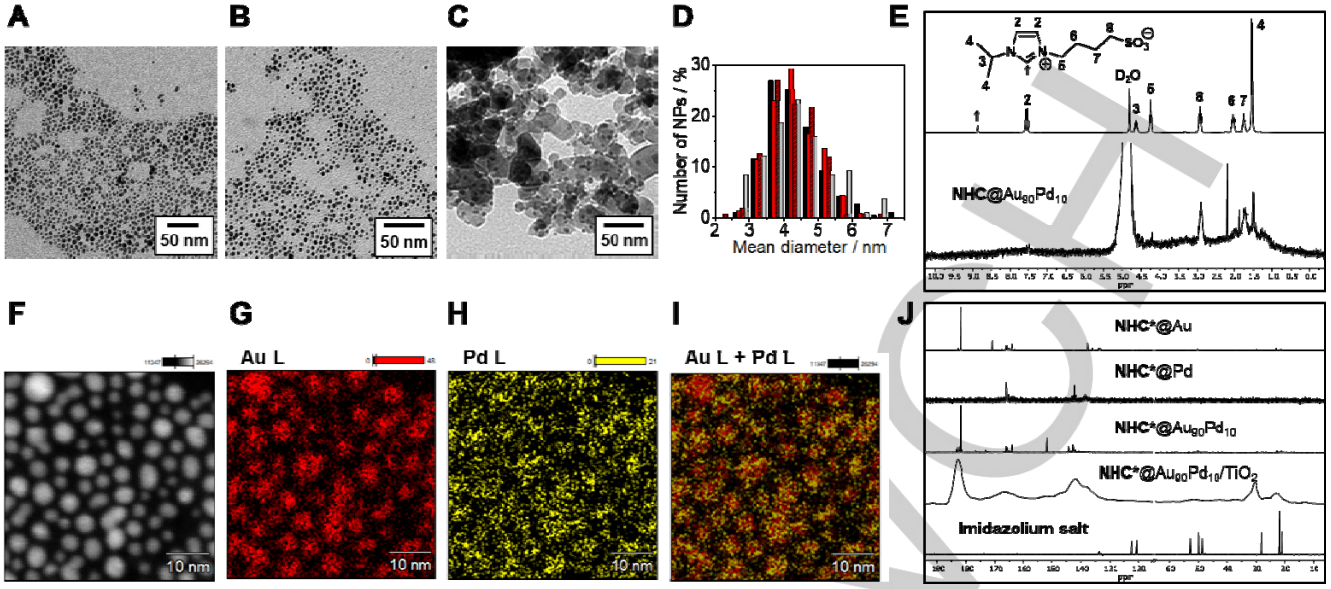

Figure 1. TEM micrographs of **OAm**@$Au_{90}Pd_{10}$ (**A**), **NHC**@$Au_{90}Pd_{10}$ (**B**), **NHC**@$Au_{90}Pd_{10}/TiO_2$ (10 wt%) (**C**) and corresponding histograms (**D**, black: **OAm**@$Au_{90}Pd_{10}$, red: **NHC**@$Au_{90}Pd_{10}$ (striped: after 3 weeks), grey: **NHC**@$Au_{90}Pd_{10}/TiO_2$). STEM-EDS micrographs of **NHC**@$Au_{90}Pd_{10}$ (**F-I**). ^{1}H NMR analysis of **NHC**@$Au_{90}Pd_{10}$ and comparison with corresponding imidazolium salt (**E**). ^{13}C NMR analysis of ^{13}C-labeled **NHC***@Au, **NHC***@Pd, **NHC***@$Au_{90}Pd_{10}$, **NHC***@$Au_{90}Pd_{10}/TiO_2$ (CPMAS) and corresponding imidazolium salt (from top to bottom) (**J**). All liquid NMR spectra were measured in D_2O.

The NHC functionalized NPs were synthesized *via* our well-established ligand exchange method[7g,7h,8a] starting from oleylamine (OAm) stabilized NPs (**OAm**@Au_xPd_y, Scheme 1). By variation of the initial Au to Pd precursor ratio the alloy NP composition can be adjusted easily.[14] The addition of the *in situ* generated free NHC and subsequent purification by dialysis for two days resulted in water-soluble NPs indicating the replacement of the hydrophobic OAm by the anionic NHC.

Deposition of the preformed NHC functionalized NPs (**NHC**@Au_xPd_y) on TiO_2 can be achieved easily by adding an aqueous solution of the NPs to a stirring aqueous suspension of the support. After only five minutes complete adsorption of the NPs became evident by coloration of the support material and the full decoloration of the supernatant after centrifugation. The prepared supported NPs (**NHC**@Au_xPd_y/TiO_2) could be suspended in all common solvents without visible leaching of the AuPd NPs up to a catalyst loading of 10 wt%.

Nanoparticle Characterization

The alloy NPs were characterized by transmission electron microscopy (TEM) confirming for all alloy NPs a mean diameter of about 4.2 nm, before and after ligand exchange reaction (Figure 1A, B; Table 1). For **NHC**@$Au_{90}Pd_{10}$ a new TEM sample was prepared from a three weeks old aqueous solution and the mean size did not change (Figure 1D). Consequently, no significant leaching of metal complexes takes place, since this would result in a decrease of the metal core size.[7e,7h] After immobilization on TiO_2, the NPs are homogenously distributed over the TiO_2 and the mean size is retained with only minor coalescence of single particles (Figure 1C). To investigate the distribution of Au and Pd in the individual NPs we measured STEM-EDS (Figure 1F-I). The elemental mapping of **NHC**@$Au_{90}Pd_{10}$ indicates a homogenous distribution of the metals and thus an alloy formation. No structural differences can be observed after NP deposition on TiO_2 or if a thiol was used instead of the NHC in the ligand exchange reaction (see the SI for details). The UV/Vis spectra of the AuPd NPs show the typical weak SPR band for Au-rich alloy NPs at ~510 nm, which was not visible for **NHC**@$Au_{75}Pd_{25}$ because of less Au-Au interactions. To gain further information on the inorganic component of the NPs, X-ray photoelectron spectroscopy (XPS) and total reflection X-ray fluorescence (TXRF) were conducted. Both methods are sensitive for surface atoms since the penetration of the X-ray decreases exponential with the depth of the analyzed material. XPS verified that both Au4f and Pd3d orbitals of the surface atoms were more electron-rich in comparison with Au(0) and Pd(0) (ΔBE ~0.6 eV, Table S2). This is typical for AuPd alloy NPs[15] and further indicates the binding of an electron donating ligand, such as a NHC. TXRF revealed an Au to Pd ratio that matches the applied metal precursor proportions for the OAm stabilized NPs (Table 1). However, after ligand exchange with the NHC ligand, the Au content seemed to increase especially for Pd-rich **NHC**@$Au_{75}Pd_{25}$ from 77 to 84%. Since a loss of Pd is unlikely due to the retained size of the particles, this finding could be explained by atom migration within the NP leading to an Au enriched surface and a Pd-rich core. A higher concentration of Au at the particle surface was also observed by Studer and coworkers for AuPd alloy NPs with similar Au:Pd ratio.[16] The surface energy of Pd is higher compared to Au, so that the rearrangement would be thermodynamically favored.[2] The trigger for the reconstruction process could be the binding of the NHC, which is known to form adatoms on Au surfaces.[6e] A similar behavior on the alloy NPs would lead to a pulling of Au atoms to the surface and would explain the Au enrichment determined by surface sensitive TXRF.

10.1002/chem.201803274

Thermogravimetric analysis (TGA) and elemental analysis revealed a similar inorganic fraction and metal-to-ligand ratio for all alloy NPs (Table 1). Nevertheless, there was a significant increase in the number of ligands with decreasing Au content, indicating a higher population of NHC ligands on surface Pd atoms. Interestingly, the values were consistently in the range between the corresponding monometallic **NHC**@Au- and PdNPs (Table 1).

Table 1. Summary of analytical data of NHC functionalized AuPd alloy NPs.

NP	Mean diameter / nm[a]	Au : Pd ratio[b]	Organic fraction[c] / %	M : L ratio[c]
OAm@$Au_{95}Pd_5$	4.2 ± 0.7	95.1 : 4.9	13.1	9.3 ± 1.1
OAm@$Au_{90}Pd_{10}$	4.3 ± 0.8	92.5 : 7.5	10.8	11.4 ± 0.8
OAm@$Au_{75}Pd_{25}$	4.2 ± 0.7	76.5 : 23.5	54.2	1.4 ± 0.4
NHC@$Au_{95}Pd_5$	4.1 ± 0.6	97.5 : 2.5	18.1	6.7 ± 0.2
NHC@$Au_{90}Pd_{10}$	4.3 ± 0.7	93.1 : 6.9	21.2	5.6 ± 0.4
NHC@$Au_{75}Pd_{25}$	4.1 ± 0.7	83.6 : 16.4	23.5	5.1 ± 0.3
NHC@Au[7h]	4.1 ± 1.6	-	8	10.0
NHC@Pd[7h]	4.1 ± 0.6	-	37	4.5
NHC@$Au_{95}Pd_5$/TiO_2	4.6 ± 0.8	-	2.8	-
NHC@$Au_{90}Pd_{10}$/TiO_2	4.3 ± 1.1	-	2.5	-
NHC@$Au_{75}Pd_{25}$/TiO_2	4.6 ± 1.1	-	2.4	-

[a] Determined by TEM. [b] Measured by TXRF. [c] Based on TGA and elemental analysis for the unsupported NPs, based on TGA for supported NPs.

^{1}H NMR analysis of the isolated NPs before and after the exchange reaction confirmed the full replacement of OAm from the NP surface since the characteristic signal of the C=C bond of OAm at 5.5 ppm was not visible in the spectra of all **NHC**@Au_xPd_y NPs (Figure 1E, S19-21). Additionally, no signal of the imidazolium salt proton (8.9 ppm) was visible, further confirming the formation of a carbene species. The observed signal broadening is characteristic for ligand stabilized MNPs and verifies the immobilization of the NHC on the NP surface.[17] To gain more structural information on the ligand shell constitution, an analogue of the NHC was synthesized which carbenic carbon atom was ^{13}C-labeled (**NHC***). This ligand was immobilized on $Au_{90}Pd_{10}$ and for comparison on monometallic Au- and PdNPs. In the ^{13}C NMR spectrum of **NHC***@$Au_{90}Pd_{10}$ several signals in the typical region for carbenic carbons were found (Figure 1J). Interestingly, signals with the same chemical shifts and splitting pattern were also observed in the spectra of **NHC***@Au- and **NHC***@PdNPs implying that the NHC binds to both the Au and Pd atoms on the alloy NP surface. We assume that the multiple hetero metal-metal bonds induce a variety of slightly different electronic states, which results in a variety of chemical shifts for the carbenic carbon atom. Additionally, nonequivalent environments of the ligands on the NPs can induce signal splitting in ^{13}C NMR as predicted by Richeter *et al.* using DFT calculations for NHC functionalized Au_{38} clusters.[7m] To investigate if some of the more defined signals might be the result of molecular metal complexes, we conducted ESI-MS measurements of **NHC***@$Au_{90}Pd_{10}$ (Figure S9,10). Different adducts from the imidazolium salt and the bis-carbene Au(I) complex were observed. Since there was no evidence for the presence of the imidazolium salt in the previous NMR experiments, we concluded that it was formed as an ionization product during the mass experiments. The binding energies for Au found *via* XPS clearly proved an oxidation state of zero in the alloy NPs. Considering this, the appearance of [Au(I)NHC_2] in the mass spectrum probably originated from fragmentation during the ionization process rather than the occurrence of complexes in the NP solution. To prove that the NHC was still bound to the alloy NP surface after immobilization on TiO_2, we conducted ^{13}C-{^{1}H} cross polarization magic-angle spinning (CPMAS) NMR experiments of **NHC***@$Au_{90}Pd_{10}$/TiO_2. The obtained spectrum showed the same signals as the ^{13}C NMR spectrum of **NHC***@$Au_{90}Pd_{10}$ in D_2O (Figure 1J), strongly indicating that the NHC remains on the alloy NP surface after immobilization.

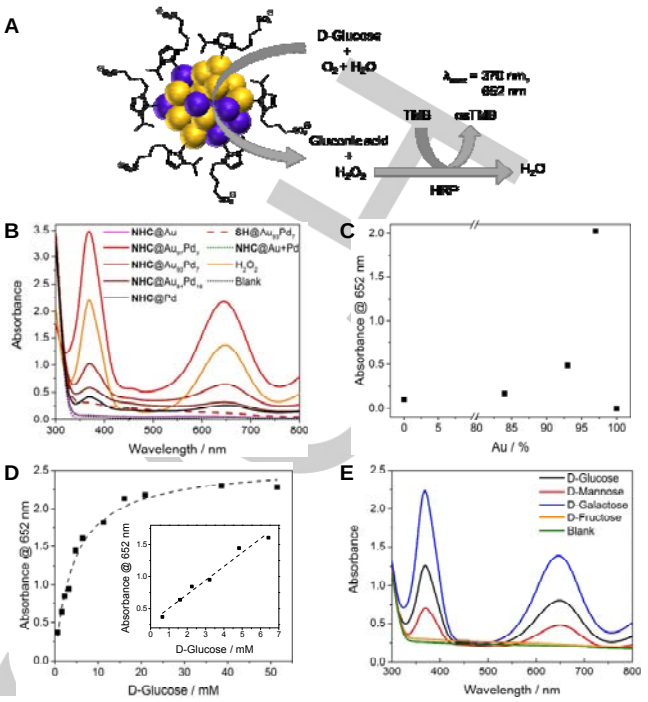

Figure 2. NHC modified AuPd alloy NPs as GOx mimic. (**A**) Schematic illustration of GOx mimicking and H_2O_2 detection with TMB. (**B**) UV/Vis spectroscopic analyses of GOx mimic properties of different AuPd alloy NPs, monometallic NPs and thiol-modified alloy NPs. (**C**) Catalytic performance of AuPd alloy NPs as a function of Au surface fraction. (**D**) Formation of oxTMB as a function of initial D-Glucose concentration with **NHC**@$Au_{90}Pd_{10}$ as catalyst. The inset shows the linear region from 0 – 7 mM D-glucose. (**E**) Aerobic oxidation of different hexoses with **NHC**@$Au_{90}Pd_{10}$ as catalysts.

Catalytic Activity

After comprehensive characterization, possible applications of the alloy NPs in catalysis were investigated. The development of

10.1002/chem.201803274

systems that feature similar catalytic activity as enzymes is an emerging research field due to the high costs and instability of natural proteins. Among these biomimetic catalysts, metal NPs are of special interest since they show interesting oxidase mimic properties.[18] Therefore, we tested the water-soluble alloy NPs as catalysts for the aerobic oxidation of D-glucose. This reaction is catalyzed in natural systems by glucose oxidase (GOx), which converts D-glucose under aerobic conditions into gluconic acid. The byproduct of this reaction (H_2O_2) can be easily assayed by the chromogenic agent tetramethylbenzidine (TMB) in combination with horseradish peroxidase (HRP) as catalyst. The combination of these two enzymatic reactions is used for quantitative glucose detection in clinical chemistry. When the alloy NPs were incubated with glucose at pH 9.2 for 30 min and the reaction solution was added to a solution containing TMB and HRP, the characteristic blue color of oxidized TMB (oxTMB, λ_{max} = 370, 652 nm) was observed, attesting to GOx-like activity. The performance of the alloys was compared among themselves and with their monometallic correspondents spectroscopically (Figure 2B). **NHC@**PdNPs show as expected no significant activity. To our surprise, in the obtained spectrum of **NHC@**AuNPs no absorbance increase at 652 nm was observed although many examples for AuNPs catalyzing the oxidation of glucose are reported.[19] A closer examination of the reaction vessel revealed visible particle aggregation on the stirring bar (Figure S9), which is likely a result of the alkaline reaction conditions and high ionic strength. We assume that the aggregates cannot function as catalyst since most of the binding sites are blocked in the agglomerates. For the alloy NPs, no aggregation was observed, which accounts their good GOx activity. Since the performance increases with higher Au content, we consider Au to be the actual active metal and the alloy effect originating from their superior colloidal stability. However, the much higher activity of $Au_{95}Pd_5$ in comparison to $Au_{90}Pd_{10}$ indicates additional, nonlinear effects influencing the catalytic properties of the alloys. When a mixture of **NHC@**Au- and PdNPs was used as catalyst (9:1) no absorbance increase at 652 nm was detected, but particle aggregation similar to the experiment with only AuNPs was observed. To find out if the NHC also has a promotional effect on the glucose conversion, we tested thiol-functionalized alloy NPs (**SH@**$Au_{90}Pd_{10}$), of which we observed no oxTMB formation. The long-chained thiol ligands might form a very dense ligand shell around the particle surface, so that the active sites would not be available for glucose. In contrast, the sterically more demanding head group and the short chain at the NHC backbone might enable substrate binding. Several groups reported before the dependence of GOx-like activity on the degree of surface coverage with ligands.[19a] Additionally, the electron-donating properties of the NHC could play a crucial role in the activity. The proposed mechanism for GOx mimicking with AuNPs described by Rossi and coworkers involves the activation of O_2 by an electron-rich Au species after glucose binding.[20] NHC ligands on the metal surface would therefore favor this key step in glucose oxidation. Variation of the initial glucose concentration with **NHC@**$Au_{90}Pd_{10}$ as catalyst demonstrated for concentrations < 7 mM a linear dependence between glucose concentration and TMB oxidation (Figure 2D). Thus, the NPs can be used potentially for glucose detection in this concentration range. Moreover, we tested other natural important hexoses as substrates to see if the oxidase mimicking was not only restricted to D-glucose. The diastereomers of D-glucose (D-mannose and D-galactose) can also be detected with the alloy NPs with good sensitivity whereas D-fructose was not oxidized (Figure 2E). In contrast to the other carbohydrates, the latter is a ketohexose, which possesses an anomeric center that is less reactive towards hydration which is important for binding

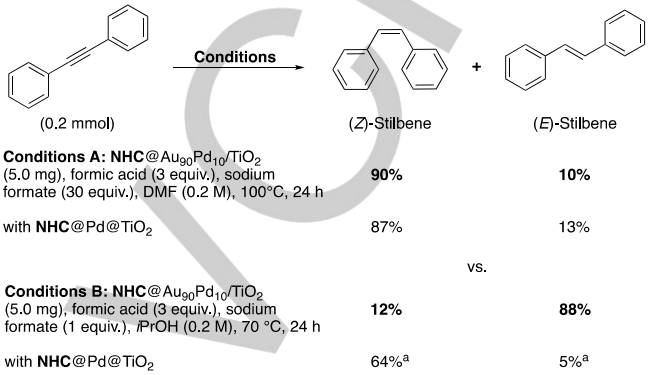

Scheme 2. (*Z*/*E*)-selective semihydrogenation of diphenylacetylene dependent from reaction conditions. [a] The reaction was performed three times and the conversion was 69%.

on the particle surface.[20]

In addition to the biomimetic catalysis in water, we further tested the catalytic activity of the NHC-modified alloys towards the semihydrogenation of diphenylacetylene via transfer hydrogenation (Scheme 2) and the hydrogenation of nitroarenes (Scheme 3). For all reactions we used **NHC@**$Au_{90}Pd_{10}/TiO_2$ which was proven to be highly active in hydrogenation reactions in initial tests and can be used in all solvents. While **NHC@**Au/TiO_2 showed no activity in all tested hydrogenation reactions, **NHC@**Pd/TiO_2 mostly showed the highest activity. However, the selectivity of the monometallic Pd-system was worse compared to the bimetallic **NHC@**$Au_{90}Pd_{10}/TiO_2$. When the transfer hydrogenation of diphenylacetylene was performed in isopropanol (3 equiv. formic acid, 1 equiv. sodium formate, 70 °C, 24 h), (*Z*/*E*)-stilbene was obtained with full conversion of the starting material in 12:88 (*Z*/*E*)-ratio. Remarkably, by slightly adjusting the reaction conditions to DMF and increasing the sodium formate equivalents (3 equiv. formic acid, 30 equiv. sodium formate, 100 °C, 24 h), we could obtain (*Z*/*E*)-stilbene, with full conversion of the starting material, in 90:10 (*Z*/*E*)-ratio. This switch in selectivity can be explained by the **NHC@**$Au_{90}Pd_{10}/TiO_2$ catalyzed semihydrogenation and subsequent isomerization of (*Z*)-stilbene to (*E*)-stilbene in polar-protic solvents such as isopropanol, which was exclusively observed for the bimetallic system and could not be observed with the monometallic **NHC@**Pd/TiO_2.

Finally, we tested the hydrogenation of nitroarenes with hydrogen gas. The reduction of the nitro-group could be obtained with low catalyst loadings under mild conditions in full conversion. While electron-donating and electron-withdrawing substituents in *para*- and *meta*-position could be readily tolerated, substituents in *ortho*-position were not tolerated.

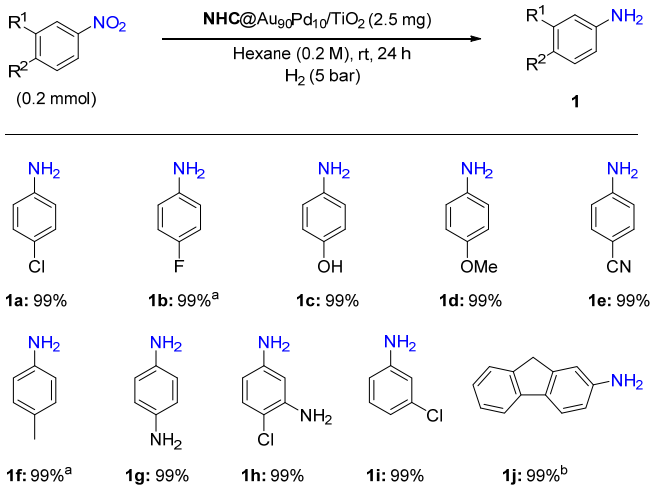

Scheme 3. Scope of the hydrogenation of nitroarenes. [a] Yield determined by GC with *n*-decane as internal standard. [b] 20 bar H_2.

Conclusions

In conclusion, AuPd alloy NPs of different metal compositions have been successfully stabilized for the first time with NHC ligands leading to monodisperse NPs with long-term stability. Extensive characterization confirmed the alloy structure of the NP core, the presence of the NHC ligand on the particle surface and electronic interactions between the metal atoms and immobilized ligands. The NHC functionalized AuPdNPs can be easily immobilized on TiO_2 as support in order to use them as recyclable catalyst. The unsupported alloy NPs exhibited high activity as catalysts in water for the oxidation of D-glucose. By far the highest conversion was observed for **NHC@**$Au_{95}Pd_5$, which can be explained by their superior colloidal stability in comparison with monometallic AuNPs. The alloy NPs on TiO_2 were successfully applied in the semi-hydrogenation of diphenylacetylene with switchable selectivity towards (*Z*)- or (*E*)-stilbene by slightly adjusting the reaction conditions. The selectivity switch can be attributed to an AuPdNP catalyzed (Z/E)-isomerization reaction in polar protic solvents. Furthermore, the supported NPs can be used as catalyst for the hydrogenation of nitroarenes under mild conditions and with low catalyst loading.

Acknowledgements

We are grateful for generous financial support by the Deutsche Forschungsgemeinschaft (SFB 858) and JSPS Core-to-Core Program “Elements Function for Transformative Catalysis and Materials”. We thank Michael Holtkamp (Institute of Inorganic and Analytical chemistry, WWU Münster) for TXRF analyses, Jessica Hüsker (MEET, WWU Münster) for TGA measurements and Dr. Melanie Brinkkötter (Institut für Physikalische Chemie, WWU Münster) for solid-state-NMR experiments. STEM-EDS measurements were conducted at High Voltage Electron Microscope Laboratory, Institute of Materials and Systems for Sustainability, Nagoya University, supported by "Nanotechnology Platform" of MEXT, Japan.

Keywords: bimetallic nanoparticles • N-heterocyclic carbenes • nanozyme • hydrogenation • transfer hydrogenation

[1] D. Astruc, in *Nanoparticles and Catalysis*, Wiley-VCH, Weinheim, Germany, **2008**, S. 1–48.
[2] A. Zaleska-Medynska, M. Marchelek, M. Diak, E. Grabowska, *Adv. Colloid Interface Sci.* **2016**, *229*, 80–107.
[3] a) F. Gao, Y. Wang, D. W. Goodman, *J. Phys. Chem. C* **2010**, *114*, 4036–4043; b) W. Luo, M. Sankar, A. M. Beale, Q. He, C. J. Kiely, P. C. A. Bruijnincx, B. M. Weckhuysen, *Nat. Commun.* **2015**, *6*, 1–10; c) R. N. Dhital, C. Kamonsatikul, E. Somsook, K. Bobuatong, M. Ehara, S. Karanjit, H. Sakurai, *J. Am. Chem. Soc.* **2012**, *134*, 20250–20253; d) S. Sarina, H. Zhu, E. Jaatinen, Q. Xiao, H. Liu, J. Jia, C. Chen, J. Zhao, *J. Am. Chem. Soc.* **2013**, *135*, 5793–5801.
[4] For reviews on NHCs in surface chemistry see: a) A. V. Zhukhovitskiy, M. J. MacLeod, J. A. Johnson, *Chem. Rev.* **2015**, *115*, 11503–11532; b) S. Engel, E.-C. Fritz, B. J. Ravoo, *Chem. Soc. Rev.* **2017**, *46*, 2057–2075.
[5] For a general review on NHCs see: M. N. Hopkinson, C. Richter, M. Schedler, F. Glorius, *Nature* **2014**, *510*, 485–496.
[6] For NHCs on flat surfaces see: a) T. Weidner, J. E. Baio, A. Mundstock, C. Große, S. Karthäuser, C. Bruhn, U. Siemeling, *Aust. J. Chem.* **2011**, *64*, 1177–1179; b) A. V. Zhukhovitskiy, M. G. Mavros, T. Van Voorhis, J. A. Johnson, *J. Am. Chem. Soc.* **2013**, *135*, 7418–7421; c) C. M. Crudden, J. H. Horton, I. I. Ebralidze, O. V Zenkina, A. B. McLean, B. Drevniok, Z. She, H. B. Kraatz, N. J. Mosey, T. Seki, E. C. Keske, J. D. Leake, A. Rousina-Webb, G. Wu, *Nat. Chem.* **2014**, *6*, 409–414; d) C. M. Crudden, J. H. Horton, M. R. Narouz, Z. Li, C. A. Smith, K. Munro, C. J. Baddeley, C. R. Larrea, B. Drevniok, B. Thanabalasingam, A. B. McLean, O. V Zenkina, I. I. Ebralidze, Z. She, H. B. Kraatz, N. J. Mosey, L. N. Saunders, A. Yagi, *Nat. Commun.* **2016**, *7*, 12654; e) G. Wang, A. Rühling, S. Amirjalayer, M. Knor, J. B. Ernst, C. Richter, H. J. Gao, A. Timmer, H. Y. Gao, N. L. Doltsinis, F. Glorius, H. Fuchs, *Nat. Chem.* **2017**, *9*, 152–156; e) H. K. Kim, A. S. Hyla, P. Winget, H. Li, C. M. Wyss, A. J. Jordan, F. A. Larrain, J. P. Sadighi, C. Fuentes-Hernandez, B. Kippelen, J.-L. Brédas, S. Barlow, S. R. Marder, *Chem. Mater.* **2017**, *29*, 3403–3411; f) C. R. Larrea, C. J. Baddeley, M. R. Narouz, N. J. Mosey, J. H. Horton, C. M. Crudden, *ChemPhysChem* **2017**, *18*, 3536–3539; g) J. F. DeJesus, M. J. Trujillo, J. P. Camden, D. M. Jenkins, *J. Am. Chem. Soc.* **2018**, *140*, 1247–1250; h) A. Lv, M. Freitag, K. M. Chepiga, A. H. Schäfer, F. Glorius, L. Chi, *Angew. Chem. Int. Ed.* **2018**, *57*, 4792–4796; i) D. T. Nguyen, M. Freitag, M. Körsgen, S. Lamping, A. Rühling, A. H. Schäfer, M. H. Siekman, H. F. Arlinghaus, W. G. van der Wiel, F. Glorius, B. J. Ravoo, *Angew. Chem. Int. Ed.* **2018**, *57*, 11465–11469.
[7] a) J. Vignolle, T. D. Tilley, *Chem. Commun.* **2009**, *37*, 7230–7232; b) E. C. Hurst, K. Wilson, I. J. S. Fairlamb, V. Chechik, *New J. Chem.* **2009**, *33*, 1837–1840; c) X. Ling, N. Schaeffer, S. Roland, M.-P. Pileni, *Langmuir* **2013**, *29*, 12647–12656; d) C. J. Serpell, J. Cookson, A. L. Thompson, C. M. Brown, P. D. Beer, *Dalton Trans.* **2013**, *42*, 1385–1393; e) M. Rodríguez-Castillo, D. Laurencin, F. Tielens, A. van der Lee, S. Clément, Y. Guari, S. Richeter, *Dalton Trans.* **2014**, *43*, 5978–5982; f) J. Crespo, Y. Guari, A. Ibarra, J. Larionova, T. Lasanta, D. Laurencin, J. M. López-de-Luzuriaga, M. Monge, M. E. Olmos, S. Richeter, *Dalton Trans.* **2014**, *43*, 15713–15718; g) C. Richter, K. Schaepe, F. Glorius, B. J. Ravoo, *Chem. Commun.* **2014**, *50*, 3204–3207; h) A. Ferry, K. Schaepe, P. Tegeder, C. Richter, K. M. Chepiga, B. J. Ravoo, F. Glorius, *ACS Catal.* **2015**, *5*, 5414–5420; i) M. J. MacLeod, J. A. Johnson, *J. Am. Chem. Soc.* **2015**, *137*, 7974–7977; j) X. Ling, N. Schaeffer, S. Roland, M.-P. P. Pileni, *Langmuir* **2015**, *31*, 12873–12882; k) X. Ling, S. Roland, M.-P. Pileni, *Chem. Mater.* **2015**, *27*, 414–423; l) S. Roland, X. Ling, M. P. Pileni, *Langmuir* **2016**, *32*, 7683–7696; m) M. Rodríguez-Castillo, G. Lugo-Preciado, D. Laurencin, F. Tielens, A. van der Lee, S. Clément, Y. Guari, J. M. López-de-Luzuriaga, M. Monge, F. Remacle, S. Richeter, *Chem. Eur. J.* **2016**, *22*, 10446–10458; n) Z. Cao, D. Kim, D. Hong, Y. Yu, J. Xu, S. Lin, X. Wen, E. M. Nichols, K. Jeong, J. A. Reimer, P. Yang, C. J. Chang, *J. Am. Chem. Soc.* **2016**, *138*, 8120–8125; o) K. Salorinne, R. W. Y. Man, C. H. Li, M. Taki, M. Nambo, C. M. Crudden, *Angew. Chem. Int. Ed.* **2017**, *56*, 6198–6202; p) M. R. Narouz, C. H. Li, A. Nazemi, C. M. Crudden, *Langmuir* **2017**, *33*, 14211–14219; q) R. W. Y. Man, C.-H. Li, M. W. A. MacLean, O. V. Zenkina, M. T. Zamora, L. N. Saunders, A. Rousina-Webb, M. Nambo, C. M. Crudden, *J. Am. Chem. Soc.* **2018**, *140*, 1576–1579.
[8] a) K. V. S. Ranganath, J. Kloesges, A. H. Schäfer, F. Glorius, *Angew.*

Chem. Int. Ed. **2010**, *49*, 7786–7789; b) A. Rühling, K. Schaepe, L. Rakers, B. Vonhören, P. Tegeder, B. J. Ravoo, F. Glorius, *Angew. Chem. Int. Ed.* **2016**, *55*, 5856–5860; c) J. M. Asensio, S. Tricard, Y. Coppel, R. Andrés, B. Chaudret, E. de Jesús, E. de Jesús, *Angew. Chem. Int. Ed.* **2017**, *56*, 865–869; d) J. M. Asensio, R. Andrés, E. de Jesús, S. Tricard, B. Chaudret, Y. Coppel, *Chem. Eur. J.* **2017**, 13435–13444.

[9] a) P. Lara, A. Suárez, V. Collière, K. Philippot, B. Chaudret, *ChemCatChem* **2014**, *6*, 87–90; b) E. A. Baquero, S. Tricard, J. C. Flores, E. De Jesffls, B. Chaudret, E. de Jesús, B. Chaudret, *Angew. Chem. Int. Ed.* **2014**, *53*, 13220–13224; c) L. M. Martínez-Prieto, L. Rakers, A. M. López-Vinasco, I. Cano, Y. Coppel, K. Philippot, F. Glorius, B. Chaudret, P. W. N. M. van Leeuwen, *Chem. Eur. J.* **2017**, *23*, 12680.

[10] a) P. Lara, O. Rivada-Wheelaghan, S. Conejero, R. Poteau, K. Philippot, B. Chaudret, *Angew. Chem. Int. Ed.* **2011**, *50*, 12080–12084; b) D. Gonzalez-Galvez, P. Lara, O. Rivada-Wheelaghan, S. Conejero, B. Chaudret, K. Philippot, P. W. N. M. van Leeuwen, *Catal. Sci. Technol.* **2013**, *3*, 99–105; c) L. M. Martínez-Prieto, A. Ferry, P. Lara, C. Richter, K. Philippot, F. Glorius, B. Chaudret, *Chem. Eur. J.* **2015**, *21*, 17495–17502; d) L. M. Martínez-Prieto, A. Ferry, L. Rakers, C. Richter, P. Lecante, K. Philippot, B. Chaudret, F. Glorius, *Chem. Commun.* **2016**, *52*, 4768–4771; e) P. Lara, L. M. Martínez-Prieto, M. Roselló-Merino, C. Richter, F. Glorius, S. Conejero, K. Philippot, B. Chaudret, *Nano-Structures & Nano-Objects* **2016**, *6*, 39–45.

[11] J. B. Ernst, S. Muratsugu, F. Wang, M. Tada, F. Glorius, *J. Am. Chem. Soc.* **2016**, *138*, 10718–10721.

[12] J. B. Ernst, C. Schwermann, G. I. Yokota, M. Tada, S. Muratsugu, N. L. Doltsinis, F. Glorius, *J. Am. Chem. Soc.* **2017**, *139*, 9144–9147.

[13] N. Möller, A. Rühling, S. Lamping, T. Hellwig, C. Fallnich, B. J. Ravoo, F. Glorius, *Angew. Chem. Int. Ed.* **2017**, *56*, 4356–4360.

[14] Ö. Metin, X. Sun, S. Sun, *Nanoscale* **2013**, *5*, 910–912.

[15] J. Xu, T. White, P. Li, C. He, J. Yu, W. Yuan, Y. Han, *J. Am. Chem. Soc.* **2010**, *132*, 10398–10406.

[16] M. Wissing, M. Niehues, B. J. Ravoo, A. Studer, *Eur. J. Org. Chem.* **2018**, 3403–3409.

[17] L. E. Marbella, J. E. Millstone, *Chem. Mater.* **2015**, *27*, 2721–2739.

[18] H. Wei, E. Wang, *Chem. Soc. Rev.* **2013**, *42*, 6060–6093.

[19] a) P. Zhou, S. Jia, D. Pan, L. Wang, J. Gao, J. Lu, J. Shi, Z. Tang, H. Liu, *Sci. Rep.* **2015**, *5*, 1–7; b) W. Luo, C. Zhu, S. Su, D. Li, Y. He, Q. Huang, C. Fan, *ACS Nano* **2010**, *4*, 7451–7458; c) Y. Zhao, Y. Huang, H. Zhu, Q. Zhu, Y. Xia, *J. Am. Chem. Soc.* **2016**, *138*, 16645–16654.

[20] M. Comotti, C. Della Pina, E. Falletta, M. Rossi, *Adv. Synth. Catal.* **2006**, *348*, 313–316.

10.1002/chem.201803274

WILEY-VCH

Entry for the Table of Contents (Please choose one layout)

Layout 1:

COMMUNICATION

It's all about the mix! The preparation of water soluble, N-heterocyclic carbene stabilized AuPd alloy nanoparticles is presented. The particles were stable over years and could be used as biomimetic catalyst in water or as heterogeneous catalysts in hydrogenation reactions.

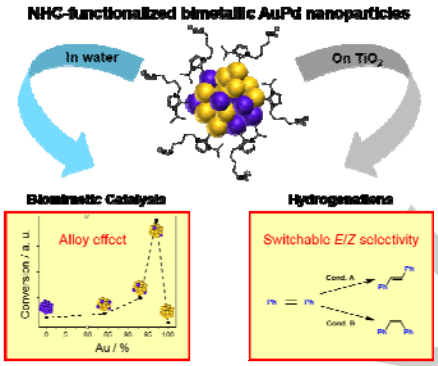

Patricia Tegeder,[+] Matthias Freitag,[+] Kathryn M. Chepiga, Satoshi Muratsugu Nadja Möller, Sebastian Lamping, Mizuki Tada, Frank Glorius and Bart Jan Ravoo**

Page No. – Page No.

N-Heterocyclic Carbene-Modified AuPd Alloy Nanoparticles and their Application as Biomimetic and Heterogeneous Catalysts